Organometallics **2007,** *26,* 6473−6480

Bimetallic Osmium−Tin Clusters: Addition of Triphenyltinhydride to Unsaturated $[Os_3(CO)_8\{\mu_3\text{-}Ph_2PCH_2P(Ph)C_6H_4\}(\mu\text{-}H)]$ and Saturated $[Os_3(CO)_{10}(\mu\text{-dppm})]$

Mohammad R. Hassan,[†] Graeme Hogarth,*[,‡] G. M. Golzar Hossain,[§] Shariff E. Kabir,*[,†]
Arun K. Raha,[†] Madhu S. Saha,[†] and Derek A. Tocher*[,‡]

Department of Chemistry, Jahangirnagar University, Savar, Dhaka-1342, Bangladesh, Department of Chemistry, University College London, 20 Gordon Street, London WC1H OAJ, United Kingdom, and Department of Chemistry, Dhaka University, Dhaka-1000, Bangladesh

Received July 30, 2007

Reaction of electron-deficient $[Os_3(CO)_8\{\mu_3\text{-}Ph_2PCH_2P(Ph)C_6H_4\}(\mu\text{-}H)]$ (**2**) with Ph_3SnH at ambient temperature yields the bimetallic osmium−tin dihydride complexes $[Os_3(CO)_8\{\mu_3\text{-}Ph_2PCH_2P(Ph)C_6H_4\}(SnPh_3)(\mu\text{-}H)_2]$ (**3**) and $[Os_3(CO)_8(\mu\text{-dppm})(SnPh_3)_2(\mu\text{-}H)_2]$ (**4**) via oxidative-addition of one and two Sn−H bonds, respectively, the latter having $SnPh_3$ ligands bound to adjacent osmium atoms. Cluster **3** converts to **4** via oxidative-addition of a further Sn−H bond followed by reductive-elimination of the orthometalated diphosphine. Heating **4** at 128 °C affords isomeric **5**, in which both the $SnPh_3$ ligands are bound to the same metal atom, and **5** is also formed from **2** and excess Ph_3SnH at 128 °C. Reaction of $[Os_3(CO)_{10}(\mu\text{-dppm})]$ (**1**), the saturated counterpart of **2**, with Ph_3SnH at 110 °C affords $[Os_3(CO)_9(\mu\text{-dppm})(SnPh_3)(\mu\text{-}H)]$ (**6**), via oxidative-addition of one Sn−H bond, and this converts to **3** upon further heating via loss of one CO followed by orthometallation of the diphosphine. Treatment of **3** with hydrogen (1 atm) at 110 °C gives both the unsaturated dihydride $[Os_3(CO)_7\{\mu_3\text{-}Ph_2PCH_2P(Ph)C_6H_4\}(SnPh_3)(\mu\text{-}H)_2]$ (**7**) and the electron-precise trihydride $[Os_3(CO)_8(\mu\text{-dppm})(SnPh_3)(\mu\text{-}H)_3]$ (**8**). Thermolysis of **8** at 110 °C gives **7**, while heating **3** in refluxing octane yields, after recrystallization from dichloromethane, the unsaturated cluster $[Os_3(CO)_7\{\mu_3\text{-}Ph_2PCH_2P(Ph)C_6H_4\}(SnPh_2Cl)(\mu\text{-}H)_2]$ (**9**), whereby the coordinated $SnPh_3$ is transformed into a $SnPh_2Cl$ group probably via Sn−Ph bond cleavage and chloride addition to the resulting $\mu\text{-}SnPh_2$ group. The crystal structures of six of these new osmium−tin clusters have been carried out, allowing a detailed analysis of the relative orientations of metal atoms.

Introduction

There continues to be considerable interest in the chemistry of transition metal−tin compounds primarily because tin is often used to modify and enhance the activity of bimetallic catalysts, leading to increasing selectivity in a variety of chemical transformations,[1−4] while there is also evidence that tin can assist in the binding of metallic nanoparticles to oxide supports when used in heterogeneous catalysis.[3−5] Group 14 metals can be incorporated into transition metal clusters in a number of ways. For example, the oxidative-addition of $R_3M'H$ to the lightly stabilized $[M_3(CO)_{12-n}(CH_3CN)_n]$ (M = Ru, Os; n = 1, 2) gives mixed metal clusters of the type $[M_3(CO)_{11}(M'R_3)(\mu\text{-}H)]$ and $[M_3(CO)_{10}(CH_3CN)(M'R_3)(\mu\text{-}H)]$ (M′ = Ge, Sn; R = Me, Et, Bu, Ph),[6] while a similar oxidative-addition of $HM'R_3$ (M′ = Si, Sn, or Ge; R = Et, Bu, Ph) to the unsaturated cluster $[Os_3(CO)_{10}(\mu\text{-}H)_2]$ affords $[Os_3(CO)_{10}(ER_3)(\mu\text{-}H)_3]$.[7] More recently, aminostannanes have also been shown to react with metal hydrides to give metal−metal bonds,[8,9] and taking advantage of this methodology, Fernández-G and Gárate-Morales have reported the formation of amine-containing osmium−tin clusters, $[Os_3(CO)_{10}(HE)(SnBu_3)(\mu\text{-}H)]$ (HE = amine), and related complexes, from the reaction of $[Os_3(CO)_{10}(\mu\text{-}H)_2]$ and aminotributylstannanes.[10]

Another method utilized for the synthesis of group 14-transition metal clusters involves the incorporation of low-valent main group metal derivatives $M'R_2$ {M′ = Sn, Ge; R =

---

* Corresponding authors. E-mail: g.hogarth@ucl.ac.uk; skabir_ju@yahoo.com.

[†] Jahangirnagar University.

[‡] University College London.

[§] Dhaka University.

[1] (a) Thomas, J. M.; Raja, R.; Lewis, D. W. *Angew. Chem., Int. Ed.* **2005**, *44*, 6456. (b) Thomas, J. M.; Johnson, B. F. G.; Raja, R.; Sankar, G.; Midgley, P. A. *Acc. Chem. Res.* **2003**, *36*, 20. (c) Thomas, J. M.; Raja, R.; Johnson, B. F. G.; Hermans, S.; Jones, M. D.; Khimyak, T. *Ind. Eng. Chem. Res.* **2003**, *42*, 1563. (d) Johnson, B. F. G. *Top. Catal.* **2003**, *24*, 147. (e) Hermans, S.; Johnson, B. F. G. *J. Chem. Soc., Chem. Commun.* **2000**, 1955.

[2] (a) Burch, R. *J. Catal.* **1981**, *71*, 348. (b) Burch, R.; Garla, L. C. *J. Catal.* **1981**, *71*, 360. (c) Srinivasan, R.; Davis, B. H. *Platinum Met. Rev.* **1992**, *36*, 151. (d) Fujikawa, T.; Ribeiro, F. H.; Somorjai, G. A. *J. Catal.* **1998**, *178*, 58.

[3] (a) Huber, G. W.; Shabaker, J. W.; Dumesic, J. A. *Science* **2003**, *300*, 2075. (b) Hermans, S.; Raja, R.; Thomas, J. M.; Johnson, B. F. G.; Sankar, G.; Gleeson, D. *Angew. Chem., Int. Ed.* **2001**, *40*, 1211. (c) Holt, M. S.; Wilson, W. L.; Nelson, J. H. *Chem. Rev.* **1989**, *89*, 11.

[4] Johnson, B. F. G.; Raynor, S. A.; Brown, D. B.; Shephard, D. S.; Mashmeyer, T.; Thomas, J. M.; Hermans, S.; Raja, R.; Sankar, G. *J. Mol. Catal. A: Chem.* **2002**, *182−183*, 89.

[5] Hungria, A.; Raja, R.; Adams, R. D.; Captain, B.; Thomas, J. M.; Midgley, P. A.; Golvenko, V.; Johnson, B. F. G. *Angew. Chem., Int. Ed.* **2006**, *45*, 969.

[6] (a) Burgess, K.; Guerin, C.; Johnson, B. F. G.; Lewis, J. *J. Organomet. Chem.* **1985**, *295*, C3. (b) Leong, W. K.; Pomeroy, R. K.; Batchelor, R. J.; Einstein, F. W. B.; Campana, C. F. *Organometallics* **1996**, *15*, 1582.

[7] (a) Hall, R. J.; Serguievski, P.; Keister, J. B. *Organometallics* **2000**, 19, 4499. (b) Einstein, F. W. B.; Pomeroy, R. K.; Willis, A. C. *J. Organomet. Chem.* **1986**, *311*, 257.

[8] Cardin, D. J.; Lappert, M. F. *J. Chem. Soc., Chem. Commun.* **1966**, 506.

[9] Cardin, D. J.; Keppie, S. A.; Lappert, M. F. *J. Chem. Soc. A* **1970**, 2594.

[10] Gràte-Morales, J. L.; Fernàndez-G, J. M. *Organometallics* **2004**, *23*, 3840.

10.1021/om7007716 CCC: $37.00

$C(SiMe_3)_2C_5H_4N\text{-}2, CH(SiMe_3)_2\}$ into transition metal clusters under mild conditions,[11,12] while bridging $SnPh_2$ ligands can also be incorporated utilizing the relatively facile cleavage of a tin−phenyl bond. In this manner, Adams et al. have reported that reactions of Ph_3SnH with metal carbonyl clusters can lead to the formation of polynuclear complexes containing large numbers of $SnPh_2$ ligands, the cleaved phenyl group being eliminated as benzene.[13−15] Thus, the high-nuclearity ruthenium−tin clusters, $[Ru_5(CO)_{10}(SnPh_3)(\mu\text{-}SnPh_2)_4(\mu_5\text{-}C)(\mu\text{-}H)]$ and $[Ru_5(CO)_7(SnPh_3)(\mu\text{-}SnPh_2)_4(C_6H_6)(\mu_5\text{-}C)(\mu\text{-}H)]$, result from reactions of $[Ru_5(CO)_{15}(\mu_5\text{-}C)]$ and $[Ru_5(CO)_{12}(C_6H_6)(\mu_5\text{-}C)]$ with excess Ph_3SnH under forcing conditions.[13a] Especially relevant to this contribution, Adams et al. have recently shown that clusters $[Os_3(CO)_{11}(SnPh_3)(\mu\text{-}H)]$ and $[Os_3(CO)_9(\mu\text{-}SnPh_2)_3]$ are formed from the reaction of $[Os_3(CO)_{12}]$ with Ph_3SnH, while also demonstrating the importance of osmium−tin interactions in multimetallic cluster synthesis. Thus, $[Os_3(CO)_9(\mu\text{-}SnPh_2)_3]$ reacts further with $[Pt(PBu^t_3)_2]$, resulting in the formation of $[Os_3(CO)_9\{Pt(PBu^t_3)_2\}(\mu\text{-}SnPh_2)_3]$ via addition of a $Pt(PBu^t_3)_2$ group across one of the osmium−tin bonds, and $[Os_3(CO)_9\{Pt(Ph)(PPh_3)_2\}(\mu\text{-}SnPh_2)_2(\mu_3\text{-}SnPh)]$ via insertion of a $Pt(PPh_3)_2$ group into one of the tin−phenyl bonds.[15]

As a result of the highly reversible orthometallation of $[Os_3(CO)_{10}(\mu\text{-dppm})]$ (**1**) (dppm = $Ph_2PCH_2PPh_2$) to give the unsaturated cluster $[Os_3(CO)_8\{\mu_3\text{-}Ph_2PCH_2P(Ph)C_6H_4\}(\mu\text{-}H)]$ (**2**) with an accessible coordination site, the latter has proven to be a pivotal precursor for the synthesis of a wide variety of interesting and potentially useful clusters. Thus, **2** reacts with CO,[16] H_2,[17] diphenylacetylene,[18] $[Au(PPh_3)][PF_6]$,[19] $[Sn\{CH(SiMe_3)_2\}_2]$,[12] phosphines,[20] thiols,[21] organic-heterothiols,[22] dithiols,[23] diazomethane,[24] PhSeSePh,[25] HX (X = Cl, Br, F),[26] and benzothiophene[27] under mild conditions. We recently reported the synthesis of the osmium−silicon clusters $[Os_3(CO)_9(\mu\text{-dppm})(SiR_3)(\mu\text{-}H)]$ and $[Os_3(CO)_7\{\mu_3\text{-}Ph_2PCH_2P(Ph)C_6H_4\}(SiR_3)(\mu\text{-}H)_2]$ (SiR_3 = $SiPh_3$, $SiEt_3$, $SiEtMe_2$) from the reaction of **2** with R_3SiH and described the dynamic behavior of the former.[28] We have now investigated the reactions of unsaturated **2** and saturated **1** with Ph_3SnH and describe the synthesis, characterization, and thermal interconversions of a series of new osmium−tin clusters.

Scheme 1

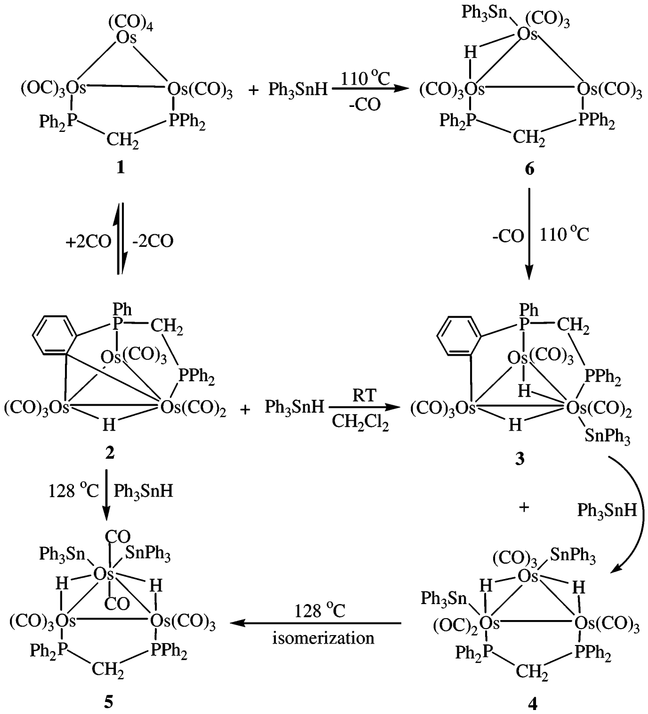

Results and Discussion

Oxidative-Addition of Ph_3Sn−H, Cluster Interconversion, and Isomerization. Treatment of a dichloromethane solution of the unsaturated cluster $[Os_3(CO)_8\{\mu_3\text{-}Ph_2PCH_2P(Ph)C_6H_4\}(\mu\text{-}H)]$ (**2**) with a slight excess of Ph_3SnH at room temperature afforded two new complexes, $[Os_3(CO)_8\{\mu_3\text{-}Ph_2PCH_2P(Ph)C_6H_4\}(SnPh_3)(\mu\text{-}H)_2]$ (**3**) and $[Os_3(CO)_8(\mu\text{-dppm})(SnPh_3)_2(\mu\text{-}H)_2]$ (**4**), in 60% and 20% yields, respectively (Scheme 1). Cluster **3** results from the oxidative-addition of one Ph_3SnH ligand to **2**, whereas **4** results from the oxidative-addition of two Ph_3SnH ligands, followed by reductive-elimination of the orthometalated phenyl group of the diphosphine ligand. In a separate experiment, it was shown that **3** is a precursor to **4**, reacting with further Ph_3SnH to give **4** in 49% yield. Under more vigorous conditions (refluxing octane), unsaturated **2** reacts with 2 equiv of Ph_3SnH to afford $[Os_3(CO)_8(\mu\text{-dppm})(SnPh_3)_2(\mu\text{-}H)_2]$ (**5**) in 40% yield, in which both of the Ph_3Sn groups are equatorially coordinated to a single metal atom (vide infra). The latter is an isomer of **4**, and heating **4** independently at 128 °C gave **5** in 46% yield, indicating that the latter is the thermodynamically most stable isomer.

---

(11) Cardin, D. J. In *Metal Clusters in Chemistry*; Braunstein, P., Oro, L. A., Raithby, P. R., Eds.; Wiley-VCH: New York, 1999; Vol. 1, p 48.

(12) (a) Cardin, C. J.; Cardin, D. J.; Convary, M. A.; Devereux, M. M. *J. Chem. Soc., Chem. Commun.* **1991**, 687. (b) Bartlett, R. A.; Cardin, C. J.; Cardin, D. J.; Lawless, G. A.; Power, J. M.; Power, P. P. *J. Chem. Soc., Chem. Commun.* **1988**, 312. (c) Cardin, C. J.; Cardin, D. J.; Lawless, G. A.; Power, J. M.; Power, M. B.; Hursthouse, M. B. *J. Organomet. Chem.* **1987**, *325*, 203. (d) Cardin, C. J.; Cardin, D. J.; Parge, H. E.; Power, J. M. *J. Chem. Soc., Chem. Commun.* **1984**, 609.

(13) (a) Adams, R. D.; Captian, B.; Fu, W.; Smith, M. D. *Inorg. Chem.* **2002**, *41*, 5593. (b) Adams, R. D.; Captain, B.; Fu, W.; Smith, M. D. *Inorg. Chem.* **2002**, *41*, 2302.

(14) Adams, R. D.; Captain, B.; Smith, J. L., Jr.; Hall, M. B.; Beddie, C. L.; Webster, C. E.; Fu, W.; Smith, M. D. *Inorg. Chem.* **2004**, *43*, 7576.

(15) Adams, R. D.; Captain, B.; Zhu, L. *Organometallics* **2006**, *25*, 2049.

(16) Clucas, J. A.; Foster, D. F.; Harding, M. M.; Smith, A. K. *J. Chem. Soc., Chem. Commun.* **1984**, 949.

(17) Clucas, J. A.; Foster, D. F.; Harding, M. M.; Smith, A. K. *J. Chem. Soc., Chem. Commun.* **1985**, 2080.

(18) Clucas, J. A.; Dolby, P. A.; Foster, D. F.; Harding, M. M.; Smith, A. K. *J. Chem. Soc., Chem. Commun.* **1987**, 1829.

(19) Harding, M. M.; Kariuki, B.; Mathews, A. J.; Smith, A. K.; Braunstein, P. *J. Chem. Soc., Dalton Trans.* **1994**, 33.

(20) (a) Brown, M. P.; Dolby, P. A.; Harding, M. M.; Mathews, A. J.; Smith, A. K. *J. Chem. Soc., Dalton Trans.* **1993**, 1671. (b) Azam, K. A.; Hursthouse, M. B.; Islam, Md. R.; Kabir, S. E.; Malik, K. M. A.; Rashid, M. A.; Sudbrake, C.; Vahrenkamp, H. *J. Chem. Soc., Dalton Trans.* **1998**, 1097. (c) Azad, S. M.; Azam, K. A.; Kabir, S. E.; Saha, M. S.; Hossain, G. M. G. *J. Organomet. Chem.* **2005**, *690*, 4206.

(21) Abedin, S. M. T.; Azam, K. A.; Hursthouse, M. B.; Kabir, S. E.; Malik, K. M. A.; Mottalib, M. A.; Rosenberg, E. *J. Cluster Sci.* **2001**, *12*, 5.

(22) Kabir, S. E.; Malik, M. M. A.; Mollah, E.; Mottalib, M. A. *J. Organomet. Chem.* **2000**, *616*, 157.

(23) Kabir, S. E.; Johns, C. A.; Malik, K. M. A.; Mottalib, M. A.; Rosenberg, E. *J. Organomet. Chem.* **2001**, *625*, 112.

(24) Abedin, S. M. T.; Hardcastle, K. I.; Kabir, S. E.; Malik, K. M. A.; Mottalib, M. A.; Rosenberg, E.; Abedin, M. J. *Organometallics* **2000**, *19*, 5623.

(25) Kabir, S. E.; Pervin, S.; Sarker, N. C.; Yesmin, A.; Sharmin, A.; Siddiquee, T. A.; Haworth, D. T.; Bennett, D. W.; Malik, K. M. A. *J. Organomet. Chem.* **2003**, *681*, 237.

(26) Kabir, S. E.; Mia, Md. A.; Sarker, N. C.; Hossain, G. M. G.; Hardcastle, K. I.; Nordlander, E.; Rosenberg, E. *J. Organomet. Chem.* **2005**, *690*, 3044.

(27) Kabir, S. E.; Mia, Md. A.; Sarker, N. C.; Hossain, G. M. G.; Hardcastle, K. I.; Nordlander, E.; Rosenberg, E. *Organometallics* **2005**, *24*, 3315.

(28) Deeming, A. J.; Hassan, Md. M.; Kabir, S. E.; Nordlander, E.; Tocher, D. A. *Dalton Trans.* **2004**, 3079.

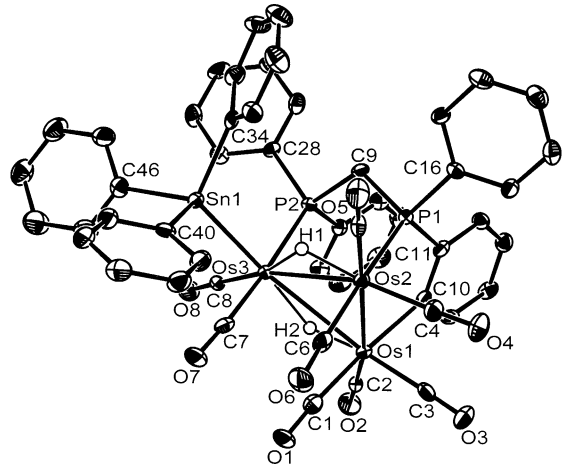

Figure 1. ORTEP diagram of $[Os_3(CO)_8\{\mu_3\text{-}Ph_2PCH_2P(Ph)C_6H_4\}(SnPh_3)(\mu\text{-}H)_2]$ (**3**) showing 30% probability thermal ellipsoids. Selected interatomic distances (Å) and angles (deg): Os(1)−Os(2) = 2.8799(3), Os(1)−Os(3) = 3.1457(3), Os(2)−Os(3) = 3.1009(3), Os(3)−Sn(1) = 2.7004(4), Os(2)−P(1) = 2.3647(15), Os(3)−P(2) = 2.4103(15), Sn(1)−Os(3)−Os(1) = 156.194(13), Sn(1)−Os(3)−Os(2) = 101.790(12), P(1)−Os(2)−Os(1) = 85.25(4), P(2)−Os(3)−Os(1) = 93.06(4).

Electron-precise $[Os_3(CO)_{10}(\mu\text{-dppm})]$ (**1**) does not react with Ph_3SnH at room temperature but in refluxing toluene gives $[Os_3(CO)_9(\mu\text{-dppm})(SnPh_3)(\mu\text{-H})]$ (**6**) in 46% yield. This cluster is formed by loss of one CO from **1** and oxidative-addition of a Ph_3SnH moiety. Upon thermolysis in refluxing toluene, **6** converts to **3** in 61% yield by further CO loss followed by orthometallation of a phenyl group of the dppm ligand. A summary of the transformations reported is shown in Scheme 1.

Clusters **3**−**6** have been characterized by a combination of spectroscopic data and single-crystal X-ray diffraction studies. The IR spectra of all compounds exhibit ν(CO) bands in the range 2085−1911 cm^{-1}, indicating that all of the carbonyl groups are terminal. The $^{31}P\{^1H\}$ NMR spectra show two doublets in the range δ −40.9 to −13.1, indicating that each contains two inequivalent phosphorus nuclei, while ^1H NMR spectra show multiplets in the aromatic region due to the phenyl protons of the dppm and triphenyltin ligands, two multiplets in the aliphatic region (δ 5.35−2.62) assigned to the diastereotopic methylene protons of the diphosphine ligand, as well as high-field resonances in the hydride region (δ −16.24 to −18.80) with $^1H-^{119}Sn$ coupling constants of 22.0−31.2 Hz. The latter are in the range previously observed for triosmium−hydride complexes containing terminally coordinated SnR_3 ligands.[15]

The molecular structure of **3** is shown in Figure 1, and selected bond distances and angles are listed in the caption. The structure consists of a triangle of osmium atoms with two similar but significantly elongated Os−Os bond distances, Os(2)−Os(3) = 3.1009(3), Os(1)−Os(3) = 3.1457(3) Å, and one shorter Os−Os bond, Os(1)−Os(2) = 2.8799(3) Å; the latter is comparable to the average Os−Os distances of 2.877(3) Å in $[Os_3(CO)_{12}]$.[29] The hydride ligands were crystallographically located (not refined) across the Os(2)−Os(3) and Os(1)−Os(3) edges.[30] The elongation of these edges is consistent with hydride-bridging. Further evidence for the hydrides was obtained from the ^1H NMR spectrum, which contains two high-field resonances at δ −16.42 and −16.75, showing coupling to phosphorus and tin: J_{PH} = 15.2 Hz, J_{SnH} = 29.0 Hz. As expected, the bulky $SnPh_3$ group is bonded terminally to one osmium atom, Os(3), the osmium−tin distance of 2.7004(4) Å being similar to those found in $[Os_3(CO)_{10}(SnMe_3)_2(\mu\text{-H})_2]$ [2.726(5) and 2.696(4) Å][31] and $[Os_3(CO)_{10}(-N{=}CH_2CH_2CH_2CH_2-)(SnBu_3)(\mu\text{-H})_2]$ [2.6929(14) Å].[10] The Os(2)−Os(3) edge is bridged by the diphosphine, the Os(3)−P(2) bond of 2.4103(15) Å being significantly longer than the Os(2)−P(1) distance of 2.3647(15) Å, while the orthometalated phenyl group binds to Os(1). Cluster **3** is electron-precise (48 valence electrons), and each osmium atom formally has an 18-electron configuration.[32]

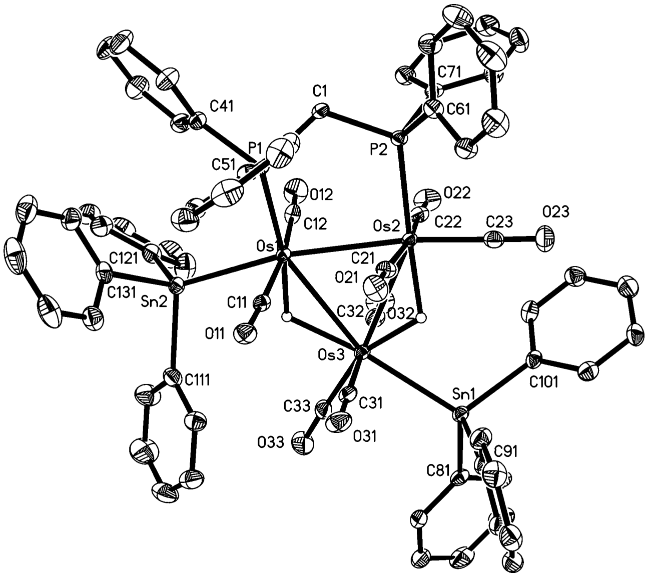

Figure 2. ORTEP diagram of $[Os_3(CO)_8(\mu\text{-dppm})(SnPh_3)_2(\mu\text{-H})_2]$ (**4**) showing 50% probability thermal ellipsoids. Selected interatomic distances (Å) and angles (deg): Os(1)−Os(2) = 2.8910(2), Os(1)−Os(3) = 3.0232(2), Os(2)−Os(3) = 3.0763(2), Os(3)−Sn(1) = 2.6977(3), Os(1)−Sn(2) = 2.6678(3), Os(1)−P(1) = 2.3069(8), Os(2)−P(2) = 2.3416(8), Sn(2)−Os(1)−Os(3) = 106.137(7), Sn(1)−Os(3)−Os(2) = 99.892(7), Sn(2)−Os(1)−Os(2) = 168.284(7), Sn(1)−Os(3)−Os(1) = 155.185(7), P(1)−Os(1)−Os(2) = 92.07(2), P(2)−Os(2)−Os(1) = 92.28(2).

The molecular structure of cluster **4** is shown in Figure 2, and selected bond distances and angles are listed in the caption. The structure consists of an isosceles triangle of osmium atoms with two significantly elongated and approximately equal [Os(2)−Os(3) = 3.0763(2), Os(1)−Os(3) = 3.0232(2) Å] and one shorter [Os(1)−Os(2) = 2.8910(2) Å] metal−metal edges. Os(1) carries two terminal carbonyl groups, while both Os(2) and Os(3) are bound to three. Hydride ligands (located and refined crystallographically) bridge across the elongated Os(2)−Os(3) and Os(1)−Os(3) edges being observed in the ^1H NMR spectrum as doublets at δ −16.24 (J = 8.4 Hz) and −17.68 (J = 28.0 Hz). The two $SnPh_3$ groups are equatorially coordinated to Os(1) and Os(3). The Os(3)−Sn(1) bond distance of 2.6977(3) Å is slightly longer than the Os(1)−Sn(2) bond distance of 2.6678(3) Å, but both are comparable to those found in **3** and $[Os_3(CO)_{10}(SnMe_3)(\mu\text{-H})_2]$ [2.6949(6) and 2.7056(4) Å].[31] The Os−P bond distances [Os(2)−P(2) = 2.3416(8) and Os(1)−P(1) = 2.3069(8) Å] are comparable to those found in **1** [2.332(3) and 2.324(4) Å].[33] Compound **4** contains 48 valence electrons, with each osmium atom having an 18-electron configuration.[32]

---

(29) Churchill, M. R.; DeBoer, B. G. *Inorg. Chem.* **1977**, *16*, 828.

(30) Teller, R. G.; Bau, R. *Struct. Bonding* **1981**, *41*, 1.

(31) Einstein, F. W. B.; Pomeroy, R. K.; Willis, A. C. *J. Organomet. Chem.* **1986**, *311*, 257.

(32) Mingos, D. M. P. *Acc. Chem. Res.* **1984**, *17*, 311.

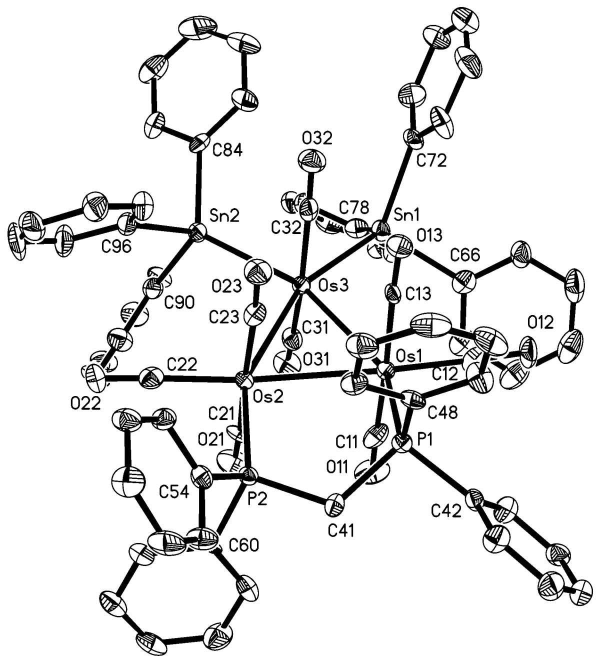

Figure 3. ORTEP diagram of $[Os_3(CO)_8(\mu\text{-dppm})(Ph_3Sn)_2(\mu\text{-}H)_2]$ (**5**) showing 50% probability thermal ellipsoids. Selected interatomic distances (Å) and angles (deg): Os(1)−Os(2) = 2.9202(4), Os(2)−Os(3) = 3.0241(4), Os(1)−Os(3) = 3.0208(3), Os(3)−Sn(1) = 2.6720(6), Os(3)−Sn(2) = 2.6653(4), Os(1)−P(1) = 2.3382(15), Os(2)−P(2) = 2.3360(16), P(1)−Os(1)−Os(2) = 89.97(4), P(2)−Os(2)−Os(1) = 93.37(4), Sn(2)−Os(3)−Sn(1) = 99.334(15), Sn(2)−Os(3)−Os(1) = 157.012(16), Sn(1)−Os(3)−Os(1) = 103.613(12), Sn(2)−Os(3)−Os(2) = 99.494(14), Sn(1)−Os(3)−Os(2) = 160.623(12).

The molecular structure of **5** is shown in Figure 3, and selected bond lengths and angles are presented in the caption. Like isomeric **4**, **5** consists of an isosceles triangle of osmium atoms with two long [Os(1)−Os(3) = 3.0208 (3) and Os(2)−Os(3) = 3.0241 (4) Å] and one comparatively shorter [Os(1)−Os(2) = 2.9202 (4) Å] metal−metal bonds and eight terminal carbonyl ligands arranged in a similar manner. The bridging hydrides were not located directly, but the lengthening of the Os(1)−Os(3) and Os(2)−Os(3) bonds indicates that they bridge these edges.[30] An interesting feature of the structure is coordination of the two bulky $SnPh_3$ groups at equatorial sites of a single metal atom, and, probably due to their large size, the angle between the $SnPh_3$ ligands at Os(3) atom is significantly greater than 90° [Sn(1)−Os(3)−Sn(2) = 99.334(15)°]. The osmium−tin bond distances [Os(3)−Sn(1) = 2.6720(6) and Os(3)−Sn(2) = 2.6653(4) Å] are comparable to those in **3** and **4**. The diphosphine bridges the Os(1)−Os(2) vector, the osmium−phosphorus bond distances [Os(1)−P(1) = 2.3382(15), Os(2)−P(2) = 2.3360(16) Å] being very similar to those observed in **1**.[32]

The molecular structure of **6** is shown in Figure 4, and selected bond lengths and angles are listed in the caption. The triosmium core in **6** represents a scalene triangle with three distinctly different metal−metal bond lengths [Os(1)−Os(3) = 3.02039(18), Os(1)−Os(2) = 2.90448(19), Os(2)−Os(3) = 2.8486(2) Å], nine terminal carbonyl ligands three bonded to each osmium atom, and a terminally coordinated $SnPh_3$ ligand. It contains one hydride ligand (located and refined crystallographically) that bridges the longest osmium−osmium edge [Os(1)−Os(3)], and, perhaps significantly, the $SnPh_3$ ligand is cis to the hydride in the sterically least crowded equatorial site. The coordination geometries of the Os atoms are approximately octahedral, the hydride occupying one of the octahedral sites at Os(1) and Os(3). In agreement with the presence of the bridging hydride ligand, the ^1H NMR spectrum exhibits a high-field resonance at δ −18.80, showing coupling to phosphorus and tin (J_{P-H} = 27.6 Hz; J_{Sn-H} = 29.0 Hz). The diphosphine bridges the intermediate Os(1)−Os(2) edge, while the shortest Os(2)−Os(3) edge is unbridged. The latter at 2.8486(2) Å is even shorter than the average osmium−osmium distance of 2.877(3) Å in $[Os_3(CO)_{12}]$. The Os(3)−Sn(1) bond of 2.6664(3) Å is comparable to those found in $[Os_3(CO)_{11}(SnPh_3)(\mu\text{-}H)]$ [2.6949(6) Å][15] and $[Os_3(CO)_{10}(-N{=}CH_2CH_2CH_2CH_2)(SnBu_3)(\mu\text{-}H)]$ [2.6929(14) Å].[10] The osmium−phosphorus bond distances [Os(2)−P(2) = 2.3122(8) and Os(1)−P(1) = 2.374(8) Å] are comparable to those in **1** [2.332(3) and 2.324(4) Å].[33] Cluster **6** contains 48 valence electrons; therefore, each osmium atom formally has an 18-electron configuration. The overall structure of **6** is similar to that of the corresponding $SiPh_3$ compound $[Os_3(CO)_9(\mu\text{-dppm})(SiPh_3)(\mu\text{-}H)]$.[28]

We have previously studied the fluxionality of $[Os_3(CO)_9(\mu\text{-dppm})(SiPh_3)(\mu\text{-}H)]$ in some detail.[28] Here, the hydride moves rapidly between the two non-diphosphine-bridged osmium−osmium vectors, while the triphenylsilyl ligand also moves between the two equatorial coordination sites. The tin analogue **6** shows very similar behavior (Scheme 2). To confirm equivalencing of the phosphorus atoms, we carried out high-resolution $^{31}P-^{31}P\{^1H\}$ exchange spectroscopy at 298 K in d_8-toluene, which clearly displayed cross-peaks between the two phosphorus signals. Changes to both the ^1H and $^{31}P\{^1H\}$ NMR spectra upon both raising (d_8-toluene) and lowering (CD_2Cl_2) the temperature were fully in accord with previous observations with $[Os_3(CO)_9(\mu\text{-dppm})(SiPh_3)(\mu\text{-}H)]$ but were made more complicated by the coupling to tin. For example, the hydride signal appeared as a doublet of doublets at 263 K (J_{PH} = 24.0, 3.2 Hz) together with eight smaller signals (tin satellites), while at 378 K it appears as a triplet (J_{PH} 15.2 H) (tin satellites unresolved). Given the close similarity to the behavior of $[Os_3(CO)_9(\mu\text{-dppm})(SiPh_3)(\mu\text{-}H)]$, we made no further attempt to probe this system.

Hydrogenation of $[Os_3(CO)_8\{\mu_3\text{-}Ph_2PCH_2P(Ph)C_6H_4\}(SnPh_3)(\mu\text{-}H)_2]$ (3), Reversal of Unsaturation, and Tin−Carbon Bond Cleavage. Both saturated **1** and unsaturated **2** react with molecular hydrogen (1 atm) at 110 °C and at ambient temperature to give unsaturated $[Os_3(CO)_8(\mu\text{-dppm})(\mu\text{-}H)_2]$. Given the facile addition of a tin−hydride bond to **3**, we decided to investigate the hydrogenation of **3** with a view to oxidatively adding hydrogen.

Reaction of **3** with H_2 (1 atm) at 110 °C leads to the formation of a mixture of the unsaturated dihydride, $[Os_3(CO)_7\{\mu_3\text{-}Ph_2PCH_2P(Ph)C_6H_4\}(SnPh_3)(\mu\text{-}H)_2]$ (**7**), and the saturated trihydride, $[Os_3(CO)_8(\mu\text{-dppm})(SnPh_3)(\mu\text{-}H)_3]$ (**8**), in 29% and 25% yields, respectively. Formation of **7** does not involve hydrogen addition; rather it results simply from loss of a carbonyl. Interestingly, thermolysis of **3** in the absence of hydrogen did not afford **7**. Formation of **8** involves hydrogen addition followed by reductive-elimination of the orthometalated phenyl group of the diphosphine ligand. In an independent experiment, cluster **8** was shown to be a precursor to **7**, the latter being transformed to **7** when a toluene solution was heated to reflux. These experiments show that initial hydrogen addition to **3** affords **8** (possibly via an unidentified tetrahydride) and this in

---

[33] Azam, K. A.; Hursthouse, M. B.; Kabir, S. E.; Malik, K. M. A.; Mottalib, M. A. *J. Chem. Crystallogr.* **1999**, *32*, 813.

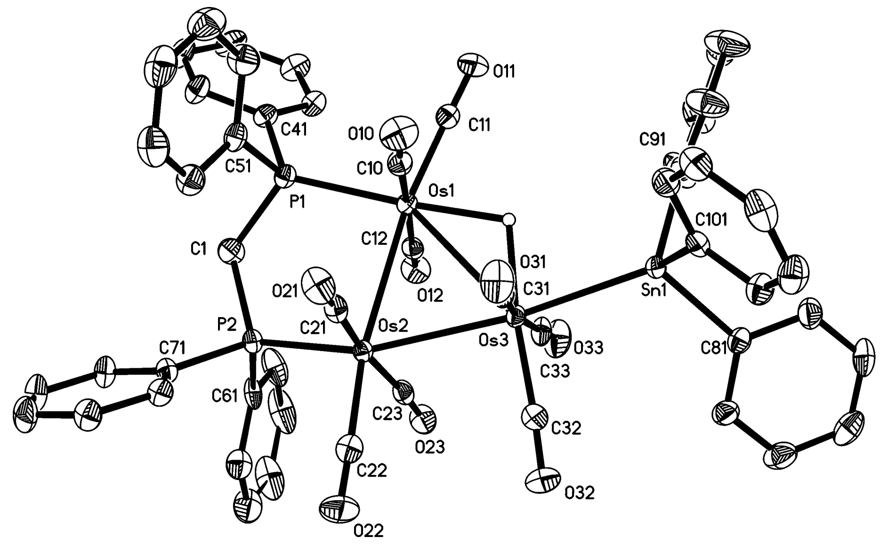

Figure 4. ORTEP diagram of [$Os_3(CO)_9(\mu$-dppm)($SnPh_3)(\mu$-H)] (**6**) showing 50% probability thermal ellipsoids. Selected interatomic distances (Å) and angles (deg): Os(1)−Os(3) = 3.02039(18), Os(1)−Os(2) = 2.90448(19), Os(2)−Os(3) = 2.8486(2), Os(3)−Sn(1) = 2.6664(3), Os(1)−P(1) = 2.3470(8), Os(2)−P(2) = 2.3122(8), P(1)−Os(1)−Os(2) = 88.60(2), P(2)−Os(2)−Os(1) = 94.37(2), Sn(1)−Os(3)−Os(2) = 173.102(7), Sn(1)−Os(3)−Os(1) = 115.183(7).

Scheme 2

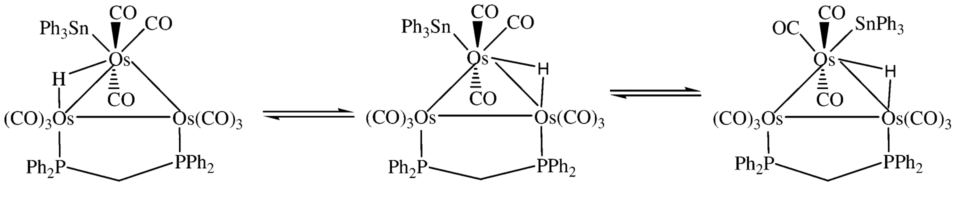

6

turn reductively eliminates hydrogen with concomitant carbonyl loss to afford **7**.

In an attempt to further probe the nature of the transformation of **3** into **7**, thermolysis of the former was carried out under more forcing conditions. Thus, after being heated at 128 °C (refluxing octane), the new cluster [$Os_3(CO)_7\{\mu_3$-Ph_2PCH_2P-(Ph)$C_6H_4\}(SnPh_2Cl)(\mu$-$H)_2$] (**9**) was isolated in 22% yield after recrystallization from dichloromethane. Formation of the Ph_2SnCl ligand in **9** is believed to involve the cleavage of a phenyl group from the coordinated Ph_3Sn ligand, which is eliminated as benzene with the formation of a bridging Ph_2Sn group. The intermediate compound with bridging Ph_2Sn moiety thus formed is most probably unstable and combines with chloride of CH_2Cl_2 during the process of workup or recrystallization, but we have not been able to confirm this. These transformations are summarized in Scheme 3. Clusters **7** and **9** have been characterized by a combination of IR, ^1H NMR, $^{31}P\{^1H\}$ NMR, and mass spectral data, together with single-crystal X-ray diffraction studies. We were unable to obtain X-ray quality crystals of **8**; therefore, its characterization is based on elemental analysis, infrared, ^1H NMR, $^{31}P\{^1H\}$ NMR, and mass spectral data.

The molecular structures of **7** and **9** are depicted in Figures 5 and 6, respectively, and selected bond distances and angles are listed in the respective captions. The structures consist of osmium triangles with two short [Os(1)−Os(2) = 2.8154(4), Os(1)−Os(3) = 2.8738(3) Å for **7** and Os(1)−Os(2) = 2.7779(3), Os(2)−Os(3) = 2.8581(3) Å for **9**] and one significantly longer [Os(2)−Os(3) = 3.0405(3) Å for **7** and Os(1)−Os(3) = 3.0156(3) Å for **9**] metal−metal bonds. The hydrides were crystallographically located and refined for **9** and found to bridge Os(1)−Os(2) and Os(1)−Os(3) edges. They were not located for **7**, but the distribution of carbonyl groups and a comparison of the bond distances and angles with those of **9** indicated that they bridge the Os(2)−Os(3) and Os(1)−Os(2) edges.

Scheme 3

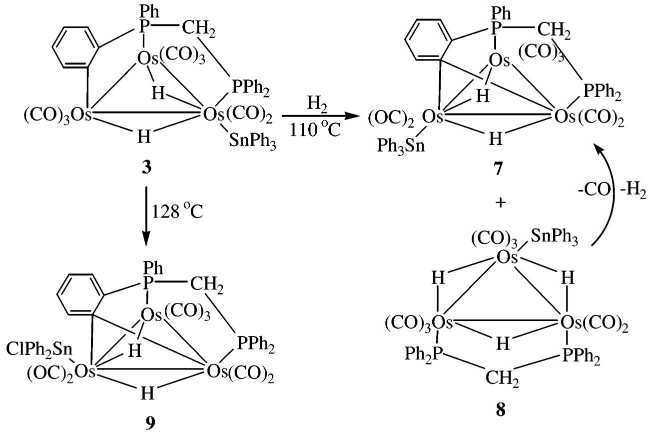

In both, the two hydrides are inequivalent and appear as doublet resonances in the ^1H NMR spectra: δ −13.56 (J = 15.5 Hz), −15.83 (J = 10.8 Hz) for **7** and δ −11.70 (J = 15.2), −13.86 (J = 13.6 Hz) for **9**. The Os(1)−Os(2) edges [2.8154(4) for **7** and 2.7779(3) Å for **9**], which are bridged by the metalated phenyl group and the hydride ligand, are significantly shorter than the other osmium−osmium distances in these two molecules and are the formal double bond character of the Os(1)−Os(2) bond, due to the formation of a three-center two-electron bond. An intriguing structural feature of both **7** and **9** is that the metalated phenyl groups form highly asymmetric bridges across the Os(1)−Os(2) edge [Os(1)−C(72) = 2.180(6), Os(2)−C(72) = 2.388(6) Å for **7**, and Os(2)−C(92) =

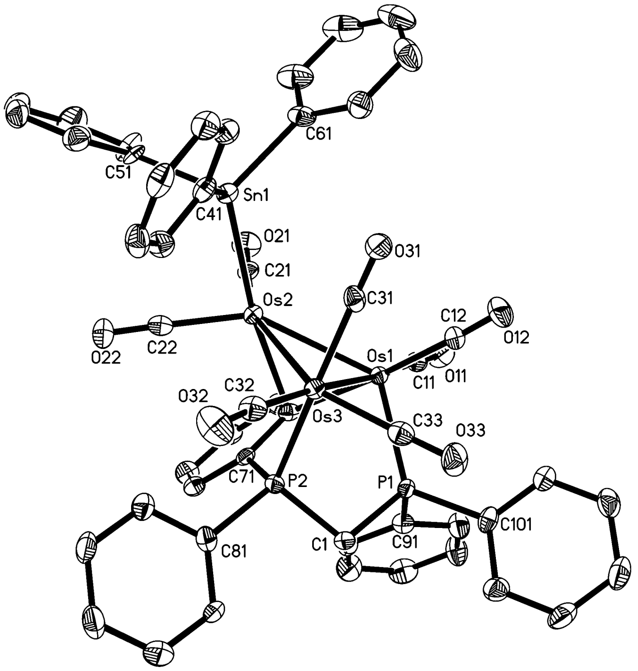

Figure 5. ORTEP diagram of $[Os_3(CO)_7\{\mu_3\text{-}Ph_2PCH_2P(Ph)C_6H_4\}(SnPh_3)(\mu\text{-}H)_2]$ (**7**) showing 50% probability thermal ellipsoids. Selected interatomic distances (Å) and angles (deg): Os(1)−Os(2) = 2.8154(4), Os(1)−Os(3) = 2.8738(3), Os(2)−Os(3) = 3.0405(3), Os(1)−P(1) = 2.3412(17), Os(3)−P(2) = 2.3432(16), Os(2)−Sn(1) = 2.6570(5), Os(2)−C(72) = 2.388(6), Os(1)−C(72) = 2.180(6), C(72)−Os(1)−Os(2) = 55.36(16), C(72)−Os(2)−Os(1) = 48.69(14), C(72)−Os(2)−Sn(1) = 172.18(15), Sn(1)−Os(2)−Os(1) = 125.098(14), Sn(1)−Os(2)−Os(3) = 99.259(13), P(2)−Os(3)−Os(1) = 76.63(4), P(1)−Os(1)−Os(3) = 91.78(4).

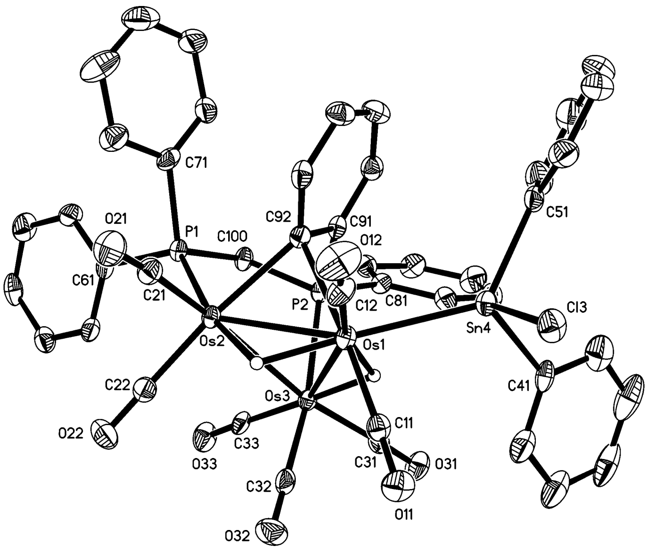

Figure 6. ORTEP diagram of $[Os_3(CO)_7\{\mu_3\text{-}Ph_2PCH_2P(Ph)C_6H_4\}(SnPh_2Cl)(\mu\text{-}H)_2]$ (**9**) showing 50% probability thermal ellipsoids. Selected interatomic distances (Å) and angles (deg): Os(1)−Os(2) = 2.7779(3), Os(1)−Os(3) = 3.0156(3), Os(2)−Os(3) = 2.8581(3), Os(1)−Sn(4) = 2.6456(4), Os(3)−P(2) = 2.3527(12), Os(2)−P(1) = 2.3458(12), Sn(4)−Cl(3) = 2.4260(13), Os(1)−C(92) = 2.347(4), Os(2)−C(92) = 2.249(5), C(92)−Os(1)−Os(2) = 51.23(11), C(92)−Os(2)−Os(1) = 54.43(11), C(92)−Os(1)−Sn(4) = 97.72(11), P(1)−Os(2)−Os(3) = 96.59(3), P(2)−Os(3)−Os(2) = 76.54(3).

2.249(5), Os(1)−C(92) = 2.347(4) Å for **9**], which is in contrast to the situation in **2**, where the corresponding osmium−carbon vectors are highly symmetrical [2.283(13) vs 2.297(13) Å]. It is notable that in both compounds **7** and **9** the long Os−C bond is observed to the osmium atom ligated by the tin. However, only in the case of **7** do the two ligands have a trans relationship. It is therefore unclear as to whether steric or electronic effects are responsible for the variation in bond lengths to the bridging carbon atom. Another interesting feature is the migration of $SnPh_3$ group from Os(3) to Os(1). The phosphorus atoms of the diphosphine ligand [Os(1)−P(1) = 2.3412(17) and Os(3)−P(2) = 2.3432(16) Å for **7** and Os(2)−P(1) = 2.3458(12) and Os(3)−P(2) = 2.3527(12) Å for **7**] are bound in a way similar to that observed for **2** [2.332(3) and 2.324(4) Å][16] and occupy axial coordination sites. The disposition of the metalated phenyl ring forces the phosphorus atoms of the diphosphine ligand to occupy axial coordination sites. Both **7** and **9** contain a total of 46 valence electrons, being two electrons short of all metal atoms having an 18-electron configuration.

The IR spectrum of $[Os_3(CO)_8(\mu\text{-dppm})(SnPh_3)(\mu\text{-}H)_3]$ (**8**) indicates that all of the carbonyl groups are terminal. In the ^1H NMR spectrum, in addition to the phenyl resonances, two multiplets centered at δ 4.03 and 4.97 are observed assigned to the inequivalent methylene protons of dppm ligand. The hydride region contains three sets of resonances each integrating for one proton: a doublet of doublets at δ −10.75 (J = 15.2 and 13.6 Hz) and two doublets at δ −12.56 (J = 9.2 Hz) and −12.93 (J = 10.4 Hz), indicating the presence of three nonequivalent bridging hydride ligands. The $^{31}P\{^1H\}$ NMR spectrum shows a singlet at δ −15.0 for two equivalent phosphorus nuclei of the dppm ligand. The FAB mass spectrum shows the molecular ion peak at m/z 1535 corresponding to the formulation of **8** and ions due to the sequential loss of eight CO groups.

Conclusions

Seven new bimetallic osmium−tin clusters containing bridging diphosphine ligands have been prepared and structurally characterized. These compounds show a sequence of steps for the transformation of the unsaturated orthometalated cluster **2** to the electron-precise dihydrido orthometalated clusters containing one and two Ph_3Sn ligands by oxidative-addition of Sn−H bonds followed by reductive-elimination of the orthometalated phenyl group. Different isomers of compounds containing two Ph_3Sn ligands have been isolated, structurally characterized, and their interconversions studied. Finally, the new bimetallic osmium−tin compounds reported in this study should be useful precursors for the preparation of new heterogeneous nanoscale catalysts on supports.

Experimental Section

General Comments. Unless otherwise stated, all reactions were performed under a nitrogen atmosphere using standard Schlenk techniques. Solvents were dried and distilled prior to use by standard methods. Ph_3SnH was purchased from Aldrich and used as received. Clusters $[Os_3(CO)_{10}(\mu\text{-dppm})]$ (**1**) and $[Os_3(CO)_8\{\mu_3\text{-}Ph_2PCH_2P(Ph)C_6H_4\}(\mu\text{-}H)]$ (**2**) were prepared according to published procedures.[16] IR spectra were recorded on a Shimadzu FTIR 8101 spectrophotometer, and ^1H and $^{31}P\{^1H\}$ NMR spectra were recorded on Varian Unity Plus 500 and Bruker DPX 400 instruments. All chemical shifts are reported in δ units with reference to the residual protons of the deuterated solvents for proton and to external 85% H_3PO_4 for ^{31}P chemical shifts. Elemental analyses were performed by the Microanalytical laboratory at University College London. Fast atom bombardment mass spectra were obtained on a JEOL SX-102 spectrometer using 3-nitrobenzyl alcohol as matrix and CsI as calibrant.

Table 1. Crystallographic Data and Structure Refinement[a] for 3, 4, 5, 6, 7, and 9

	3	**4**·2CH$_2$Cl$_2$	**5**	**6**	**7**	**9**·CH$_2$Cl$_2$
empirical formula	$C_{51}H_{38}O_8Os_3P_2Sn$	$C_{71}H_{58}Cl_4O_8Os_3P_2Sn_2$	$C_{69}H_{52}O_8Os_3P_2Sn_2$	$C_{52}H_{38}O_9Os_3P_2Sn$	$C_{50}H_{39}O_7Os_3P_2Sn$	$C_{45}H_{35}Cl_3O_7Os_3P_2Sn$
fw	1572.51	2050.89	1879.03	1558.05	1503.04	1545.31
temp (K)	150(2)	150(2)	293(2)	150(2)	150(2)	150(2)
wavelength (Å)	0.71073	Mo Kα, 0.71073	Mo Kα, 0.71073	Mo Kα, 0.71073	Mo Kα, 0.71073	Mo Kα, 0.71073
cryst syst	triclinic	triclinic	orthorhombic	monoclinic	monoclinic	triclinic
space group	$P\bar{1}$	$P\bar{1}$	*Pbca*	$P2_1/c$	$P2_1/c$	$P\bar{1}$
unit cell dimensions						
a, Å	10.90400(10)	14.2329(8)	14.9950(7)	19.3424(9)	14.3860(8)	10.4224(7)
b, Å	12.88450(10)	15.4458(9)	22.2999(11)	10.1958(5)	21.5353(12)	12.2501(8)
c, Å	19.9086(3)	16.8714(9)	37.5654(18)	25.7302(12)	15.5179(9)	18.9398(12)
α, deg	92.8510(4)	73.5330(10)	90	90	90	100.6550(10)
β, deg	91.9510(5)	89.0550(10)	90	101.2690(10)	109.7104(10)	105.4210(10)
γ, deg	114.4841(8)	76.4530(10)	90	90	90	93.5390(10)
volume, Å^3	2 537 073(5)	3452.9(3)	12 561.4(10)	4976.5(4)	4525.8(4)	2275.1(3)
Z	2	2	8	4	4	2
D_{calc}, g cm^{-3}	2.058	1.973	1.987	2.080	2.206	2.256
μ (Mo Kα), mm^{-1}	8.140	6.468	6.937	8.250	9.064	9.189
F(000)	1474	1948	7104	2920	2812	1440
crystal size, mm	0.15 × 0.12 × 0.10	0.53 × 0.31 × 0.24	0.40 × 0.11 × 0.03	0.34 × 0.22 × 0.18	0.49 × 0.44 × 0.04	0.31 × 0.13 × 0.07
θ range, deg	2.19−27.47	1.60−28.29	1.72−28.34	1.61−28.29	1.68−28.29	1.70−28.31
index ranges	$-14 \le h \le 14$ $-16 \le k \le 16$ $-25 \le l \le 25$	$-18 \le h \le 18$ $-19 \le k \le 20$ $-22 \le l \le 22$	$-19 \le h \le 19$ $-29 \le k \le 29$ $-50 \le l \le 49$	$-25 \le h \le 25$ $-13 \le k \le 13$ $-33 \le l \le 33$	$-18 \le h \le 18$ $-28 \le k \le 28$ $-20 \le l \le 20$	$-13 \le h \le 13$ $-16 \le k \le 16$ $-25 \le l \le 25$
reflns collected	44 484	30 814	107 523	43 112	38 003	20 304
independent reflns	11 522 [*R*(int) = 0.0774]	15 959 [*R*(int) = 0.0207]	15 304 [*R*(int) = 0.2511]	11 927 [*R*(int) = 0.0302]	10 785 [*R*(int) = 0.0646]	10 518 [*R*(int) = 0.0277]
reflns with $F^2 > 2\sigma$		14 808	13 278	11 027	9954	9308
max. and min. transmn	0.4966 and 0.3748	0.1309 and 0.3047	0.1679 and 0.8189	0.1630 and 0.3136	0.0952 and 0.7132	0.1599 and 0.5656
weighting parameters *a*, *b*		0.0389, 7.2106	0.0097, 31.0342	0.0246, 3.9167	0.0440, 9.8238	0.0241, 2.0286
data/restraints/parameters	11 522/6/622	15 959/0/817	15 304/0/757	11 927/2/607	10 785/0/568	10 518/0/558
GOF on F^2	1.027	0.838	1.112	1.008	1.079	1.021
final *R* indices [$I > 2\sigma(I)$]	$R_1 = 0.0377$ $wR_2 = 0.0831$	$R_1 = 0.0236$ $wR_2 = 0.0582$	$R_1 = 0.0463$ $wR_2 = 0.1059$	$R_1 = 0.0212$ $wR_2 = 0.0498$	$R_1 = 0.0460$ $wR_2 = 0.1142$	$R_1 = 0.0290$ $wR_2 = 0.0624$
R indices (all data)	$R_1 = 0.0477$ $wR_2 = 0.0874$	$R_1 = 0.0261$ $wR_2 = 0.0597$	$R_1 = 0.0549$ $wR_2 = 0.1100$	$R_1 = 0.0244$ $wR_2 = 0.0509$	$R_1 = 0.0497$ $wR_2 = 0.1171$	$R_1 = 0.0351$ $wR_2 = 0.0645$
largest diff peak and hole, e Å^{-3}	1.849 and −2.150	1.705 and −1.288	3.001 and −2.522	1.511 and −1.264	4.527 and −3.060	1.528 and −0.929

[a] Details in common, X-radiation, Mo Kα (λ = 0.71073 Å); refinement method, full-matrix least-squares on F^2.

Reaction of [$Os_3(CO)_8$\{μ_3-$Ph_2PCH_2P(Ph)C_6H_4$\}(μ-H)] (2) with Ph_3SnH. (a) At Room Temperature. To a dichloromethane solution (20 mL) of **2** (44 mg, 0.037 mmol) was added Ph_3SnH (20 mg, 0.057 mmol), and the reaction mixture was stirred at room temperature for 4 h until the color changed from green to yellow. The solvent was removed under reduced pressure, and the residue chromatographed by TLC on silica gel. Elution with hexane/CH_2Cl_2 (7:3, v/v) developed two bands. The faster moving band afforded [$Os_3(CO)_8$\{μ_3-$Ph_2PCH_2P(Ph)C_6H_4$\}($SnPh_3$)(μ-H)$_2$] (**3**) (33 mg, 60%) as pale yellow crystals after recrystallization from CH_2Cl_2/hexane at −4 °C. Anal. Calcd for $C_{51}H_{38}O_8Os_3P_2Sn$: C, 40.03; H, 2.50. Found: C, 40.28; H, 2.65. IR (νCO, CH_2Cl_2): 2081 vs, 2044 vs, 2025 vs, 1987 br, 1969 br cm^{-1}. ^{1}H NMR ($CDCl_3$): δ 6.91−7.65 (m, 30H), 6.72 (m, 1H), 6.52 (m, 1H), 6.45 (m, 1H), 6.26 (m, 1H), 4.43 (m, 1H), 2.62 (m, 1H), −16.75 (d, *J* = 15.2 Hz, 1H, J_{SnH} = 13.6 Hz), −16.42 (m, 1H, J_{SnH} = 19.2 Hz). ^{31}P\{^{1}H\} NMR ($CDCl_3$): δ −13.1 (d, *J* = 49.7 Hz), −20.96 (d, *J* = 49.7 Hz). FAB MS: *m/z* 1530. The slower moving band gave [$Os_3(CO)_8$(μ-dppm\}($SnPh_3$)$_2$(μ-H)$_2$] (**4**) (12 mg, 20%) as yellow crystals from CH_2Cl_2/hexane at −4 °C. Anal. Calcd for $C_{69}H_{54}O_8Os_3P_2Sn_2$: C, 44.05; H, 2.89. Found: C, 44.28; H, 2.88. IR (νCO, CH_2Cl_2): 2096 w, 2054 s, 2017 vs, 1998 vs, 1911 br cm^{-1}. ^{1}H NMR ($CDCl_3$): δ 6.76−7.53 (m, 50H), 5.33 (m, 1H), 4.88 (m, 1H), −16.24 (d, *J* = 6.4 Hz, 1H, J_{SnH} = 21.4 Hz), −17.68 (d, *J* = 18.0 Hz, 1H, J_{SnH} = 23.8 Hz). ^{31}P\{^{1}H\} NMR ($CDCl_3$): δ −36.9 (d, *J* = 28.5 Hz), −20.2 (d, *J* = 28.5 Hz). FAB MS: *m/z* 1882.

(b) At 128 °C. An octane suspension (20 mL) of **2** (30 mg, 0.024 mmol) and Ph_3SnH (18 mg, 0.048 mmol) was heated to reflux at 128 °C for 5 h. The solvent was removed under reduced pressure, and the residue was chromatographed by TLC on silica gel. Elution with hexane/CH_2Cl_2 (7:3, v/v) developed only one band, which afforded [$Os_3(CO)_8$(μ-dppm)($SnPh_3$)$_2$(μ-H)$_2$] (**5**) (22 mg, 46%) as pale yellow crystals after recrystallization from CH_2Cl_2/hexane at −4 °C. Anal. Calcd for $C_{69}H_{52}O_8Os_3P_2Sn_2$: C, 44.10; H, 2.79. Found: C, 44.35; H, 2.87. IR (νCO, CH_2Cl_2): 2053 s, 2012 vs, 1995 vs, 1935 w cm^{-1}. ^{1}H NMR ($CDCl_3$): δ 6.38−7.70 (m, 50H), 5.31 (m, 1H), 4.87 (m, 1H), −16.29 (d, *J* = 15.6 Hz, 1H, J_{SnH} = 20.4 Hz), −17.70 (d, *J* = 15.6 Hz, 1H, J_{SnH} = 22.4 Hz). ^{31}P\{^{1}H\} NMR ($CDCl_3$): δ −36.7 (d, *J* = 25.0 Hz), −20.5 (d, *J* = 25.0 Hz). FAB MS: *m/z* 1880.

Reaction of [$Os_3(CO)_{10}$(μ-dppm)] (1) with Ph_3SnH. A toluene solution (20 mL) of **1** (25 mg, 0.021 mmol) and Ph_3SnH (20 mg, 0.057 mmol) was refluxed for 4 h. The solvent was removed by rotary evaporation, and the residue chromatographed by TLC on silica gel. Elution with hexane/CH_2Cl_2 (7:3, v/v) developed only one band, which afforded [$Os_3(CO)_9$(μ-dppm)($SnPh_3$)(μ-H)] (**6**) (15 mg, 46%) as yellow crystals from hexane/CH_2Cl_2 at −4 °C. Anal. Calcd for $C_{52}H_{38}O_9Os_3P_2Sn$: C, 40.08; H, 2.46. Found: C, 40.20; H, 2.62. IR (νCO, CH_2Cl_2): 2085 w, 2045 vs, 2004 vs, 1977 s, 1964 w, 1879 w cm^{-1}. ^{1}H NMR ($CDCl_3$): δ 7.11−7.63 (m, 35H), 5.35 (t, *J* = 10.9 Hz, 2H), −18.80 (dd, *J* = 24.0, 3.2 Hz, 1H, J_{SnH} = 25.4 Hz). ^{31}P\{^{1}H\} NMR ($CDCl_3$): δ −30.0 (d, *J* = 28.5 Hz), −40.9 (d, *J* = 28.5 Hz). FAB MS: *m/z* 1558.

Reaction of 3 with Ph_3SnH. A dichloromethane solution (10 mL) of **3** (20 mg, 0.011mmol) and Ph_3SnH (12 mg. 0.034 mmol) was stirred at room temperature for 10 h. The solvent was removed under reduced pressure, and the residue chromatographed as above to give unconsumed **3** (2 mg, 10%) and **4** (12 mg, 49%).

Reactions of [$Os_3(CO)_8$\{μ_3-$Ph_2PCH_2P(Ph)C_6H_4$\}($SnPh_3$)(μ-H)$_2$] (3) with H_2. Hydrogen gas was bubbled through a refluxing toluene solution (20 mL) of **3** (50 mg, 0.033 mmol) for 1 h. The solvent was removed under reduced pressure, and the residue chromatographed by TLC on silica gel. Elution with hexane/CH_2Cl_2 (7:3, v/v) developed two bands. The first band afforded [$Os_3(CO)_7$\{$Ph_2PCH_2P(Ph)C_6H_4$\}($SnPh_3$)(μ-H)$_2$] (**7**) (18 mg, 29%) as orange crystals after recrystallization from CH_2Cl_2/hexane at

−4 °C. Anal. Calcd for $C_{50}H_{39}O_7Os_3P_2Sn$: C, 39.95; H, 2.62. Found: C, 40.22; H, 2.85. IR (νCO, CH_2Cl_2): 2112 w, 2068 vs, 2053 s, 2012 vs, 1993 vs, 1945 s cm^{-1}. ^{1}H NMR ($CDCl_3$): δ 7.85−5.99 (m, 34H), 4.85 (m, 1H), 3.79 (m, 1H), −13.56 (d, J = 15.5 Hz, 1H, J_{SnH} = 26.4 Hz), −15.83 (d, J = 10.8 Hz, 1H, J_{SnH} = 24.4 Hz). $^{31}P\{^{1}H\}$ NMR ($CDCl_3$): δ −14.8 (d, J = 62.8 Hz), −19.8 (d, J = 62.8 Hz). FAB MS: m/z 1503. The second band afforded $[Os_3(CO)_8(\mu\text{-dppm})(SnPh_3)(\mu\text{-}H)_3]$ (**8**) (18 mg, 25%) as yellow crystals after recrystallization from CH_2Cl_2/hexane at −4 °C. Anal. Calcd for $C_{51}H_{40}O_8Os_3P_2Sn$: C, 39.98; H, 2.63. Found: C, 40.27; H, 2.75. IR (νCO, CH_2Cl_2): 2066 vs, 2051 s, 2010 vs, 1991 vs, 1943 s cm^{-1}. ^{1}H NMR ($CDCl_3$): δ 7.84−6.1 (m, 33H), 4.97 (m, 1H), 4.03 (m, 1H), −10.75 (dd, J = 15.2, 13.6 Hz, 1H), −12.56 (d, J = 9.2 Hz, 1H), −12.93 (d, J = 10.4 Hz, 1H) (tin satellites not resolved). $^{31}P\{^{1}H\}$ NMR ($CDCl_3$): δ −14.8 (s). FAB MS: m/z 1532.

Thermolysis of 3. An octane suspension (10 mL) of **3** (40 mg, 0.027 mmol) was refluxed for 4 h, during which time the color changed from pale yellow to red. A chromatographic separation similar to that above afforded $[Os_3(CO)_7\{\mu_3\text{-}Ph_2PCH_2P(Ph)\text{-}C_6H_4\}(SnPh_2Cl)(\mu\text{-}H)_2]$ (**9**) (11 mg, 22%) as red crystals. Anal. Calcd for $C_{44}H_{33}O_7Os_3P_2SnCl$: C, 36.18; H, 2.28. Found: C, 36.34; H, 2.43. IR (νCO, CH_2Cl_2): 2070 vs, 2024 vs, 2000 vs, 1958 s, 1937 w cm^{-1}. ^{1}H NMR ($CDCl_3$): δ 7.84−6.97 (m, 25H), 6.15−6.43 (m, 4H), 4.92 (m, 1H), 4.13 (m, 1H), −11.70 (d, J = 15.2 Hz, 1H, J_{SnH} = 27.4 Hz), −13.86 (d, J = 13.6 Hz, 1H, J_{SnH} = 24.8 Hz). $^{31}P\{^{1}H\}$ NMR ($CDCl_3$): δ −15.5 (d, J = 45.5 Hz), −19.4 (d, J = 45.5 Hz). FAB MS: m/z 1460.

Conversion of 4 to 5. An octane solution (15 mL) of **4** (25 mg, 0.013 mmol) was refluxed for 3 h, during which time the color changed to pale yellow. The solvent was removed under reduced pressure, and the residue chromatographed as above to give **5** (14 mg, 56%) and unconsumed **4** (5 mg, 20%).

Conversion of 8 to 7. A toluene solution (10 mL) of **8** (41 mg, 0.027 mmol) was refluxed for 4 h. The solvent was rotary evaporated, and the residue chromatographed as above to give **7** (28 mg, 56%).

Conversion of 6 to 3. A toluene solution (8 mL) of **6** (25 mg, 0.016 mmol) was refluxed for 12 h. The solvent was rotary evaporated, and the residue was chromatographed as above to give **3** (15 mg, 61%).

X-ray Crystallography. Single crystals of **3**, **4**, **5**, **6**, **7**, and **9** suitable for X-ray diffraction were grown by slow diffusion of hexane into a dichloromethane solution at −4 °C. All geometric and crystallographic data for **4**, **6**, **7**, and **9** were collected at 150 K and for **5** at 293 K on a Bruker SMART APEX CCD diffractometer using Mo Kα radiation (λ = 0.71073 Å). Data reduction and integration was carried out with SAINT+, and absorption corrections were applied using the program SADABS.[34] Structures were solved by direct methods and developed using alternating cycles of least-squares refinement and difference Fourier synthesis. All non-hydrogen atoms were refined anisotropically. Hydrogen atoms, except those bonded to Os, were placed in the calculated positions and their thermal parameters linked to those of the atoms to which they were attached (riding model). Hydrogen atoms bridging Os atoms were located, and their positions were refined for compounds **4**, **6**, and **9** using fixed isotropic thermal parameters. The SHELXTL PLUS V6.10 program package was used for structure solution and refinement.[35] Final difference maps did not show any residual electron density of stereochemical significance. The details of the data collection and structure refinement are given in Table 1.

Intensity data for **3** were collected at 150 K, using a Bruker Nonious Kappa CCD diffractometer using Mo Kα radiation (λ = 0.71073 Å). Data collection and processing were carried out using the programs COLLECT[36] and DENZO.[37] Data were corrected for absorption effects using SORTAV.[38,39] The structure was solved by direct methods (SHELXS-97)[40] and refined on F^2 by full matrix least-squares (SHELXL-97)[41] using all unique data. The bridging hydrides were located from a difference map but not refined. All non-hydrogen atoms were refined anisotropically. The hydrogen atoms were included in calculated positions (riding model) with U_{iso} set at 1.2 times the U_{eq}.

Acknowledgment. Part of this work was carried out by S.E.K. at University College London. S.E.K. gratefully acknowledges the Royal Society (London) for a fellowship to spend time at UCL. We thank Professor A. J. Deeming for X-ray diffraction data collection for compound **7**.

Supporting Information Available: CIF files giving X-ray crystallographic data for **3**−**7** and **9**. This material is available free of charge via the Internet at http://pubs.acs.org. Crystallographic data for the structural analyses have been deposited with the Cambridge Crystallographic Data Centre, CCDC nos. 648039 for **3**, 650817 for **4**, 650820 for **5**, 650818 for **6**, 650819 for **7**, and 650816 for **9**. Copies of this information may be obtained free of charge from The Director, CCDC, 12 Union Road, Cambridge, CB2 1EZ, UK (fax, +44 1223 336033; e-mail, deposit@ccdc.cam.ac.uk; or website, http://www.ccdc.ac.uk).

OM7007716

---

(34) *SMART and SAINT+ software for CCDC diffractometers*, version 6.1; Bruker AXS Inc.: Madison, WI, 2000.

(35) Sheldrick, G. M. *SHELXTL PLUS*, version 6.1; Bruker AXS: Madison, WI, 2000.

(36) Hooft, R. *COLLECT: Data Collection Software*; Nonius B. V.: Deft, The Netherlands, 1988.

(37) Otwinowski, Z.; Minor, W. In *Macromolecular Crystallography*; Carter, C. W., Jr., Sweet, R. M., Eds.; Academic Press: New York, 1997; pp 307−326.

(38) Blessing, R. H. *Acta Crystallogr.* **1995**, *51A*, 33.

(39) Blessing, R. H. *J. Appl. Crystallogr.* **1997**, *30*, 421.

(40) Blessing, R. H. *Acta Crystallogr.* **1990**, *46A*, 467.

(41) Sheldrick, G. M. *SHELXL-97, Program for Crystal Structure Refinement*; University of Göttingen: Göttingen, Germany, 2003.